



Modeling ventricular repolarization gradients in normal cases using the equivalent dipole layer

M. Kloosterman^{a,*}, M.J. Boonstra^a, I. van der Schaaf^a, P. Loh^a, P.M. van Dam^{a,b}

^a Department of Cardiology, University Medical Center Utrecht, Heidelberglaan 100, 3584, CX, Utrecht, the Netherlands,

^b ECG Excellence, Weijland 38, 2415 BC Nieuwerbrug, the Netherlands.

ARTICLE INFO

Keywords:

Ventricular repolarization gradients
Equivalent dipole layer
Body surface potential mapping
Electrocardiographic imaging

ABSTRACT

Background Electrical activity underlying the T-wave is less well understood than the QRS-complex. This study investigated the relationship between normal T-wave morphology and the underlying ventricular repolarization gradients using the equivalent dipole layer (EDL).

Methods Body-surface-potential-maps (BSPM, 67-leads) were obtained in nine normal cases. Subject specific MRI-based anatomical heart/torso-models with electrode positions were created. The boundary element method was used to account for the volume conductor effects. To simulate the measured T-waves, the EDL was used to apply different ventricular repolarization gradients: a) transmural, b) interventricular c) apico-basal and d) all three gradients (a-c) combined. The combined gradient (d) was optimized using an inverse procedure (Levenberg-Marquardt). Correspondence between simulated and measured T-waves was assessed using correlation coefficient (CC) and relative difference (RD).

Results Realistic T-waves were simulated if repolarization times of: (a) the epicardium were smaller than the endocardium; (b) the left ventricle were smaller than the right ventricle and (c) the apex increased towards the base. The apico-basal gradient resulted in the highest correspondence between measured and simulated T-waves (CC = 0.84(0.81–0.91); RD = 0.68(0.60–0.71)) compared to a transmural gradient (CC = 0.77(0.71–0.80); RD = 1.46(0.82–1.75)) and an interventricular gradient (CC = 0.71(0.67–0.80); RD = 0.85(0.75–0.87)). All three gradients combined further improved the correspondence between measured and simulated T-waves (CC = 0.83(0.82–0.89); RD = 0.60(0.51–0.63)), especially after optimization (CC = 0.96(0.94–0.98); RD = 0.27(0.22–0.34)).

Conclusion The application of all repolarization gradients combined resulted in the largest agreement between simulated and measured T-waves, followed by the apico-basal repolarization gradient. With these findings, we will optimize our EDL-based inverse procedure to assess repolarization abnormalities.

Introduction

The electrocardiogram (ECG) is widely used as a diagnostic tool to provide insight in the electrical activity of the heart. The shape and magnitude of the measured body surface potentials can change over time due to the development of cardiac disease. Abnormalities can then be identified in both the depolarization and repolarization phase of the ECG. For example, fragmentation of the QRS complex indicates the presence of myocardial conduction delays within the depolarization phase. [1] For the repolarization phase, inverted T-waves can be a sign of myocardial ischemia. [2] However, the underlying pathological mechanism of these T-wave changes is less well understood compared to waveform changes within the depolarization phase. [3,4]

The genesis of the T-wave is a result of local repolarization heterogeneities in the ventricular myocardium. Both the temporal and spatial differences are responsible for repolarization gradients resulting in the shape of the T-wave. [3–5] However, there is a lot of controversy in literature about those temporal and spatial repolarization gradients. [4] This may be explained by the differences in applied models: computerized models, whole heart studies, wedge preparations and cell clamp studies, but also the studied subjects: human, canine and porcine hearts. [3,6]

An interventricular, transmural and apico-basal repolarization gradient have been described in literature to be the main ventricular gradients in humans resulting in the T-wave. [4–6] These ventricular repolarization gradients were therefore simulated in this study using the

* Corresponding author.

E-mail address: manon.kloosterman@live.com (M. Kloosterman).

<https://doi.org/10.1016/j.jelectrocard.2023.11.003>

Received 2 June 2023; Received in revised form 20 September 2023; Accepted 5 November 2023

Available online 14 November 2023

0022-0736/© 2023 The Authors. Published by Elsevier Inc. This is an open access article under the CC BY license (<http://creativecommons.org/licenses/by/4.0/>).

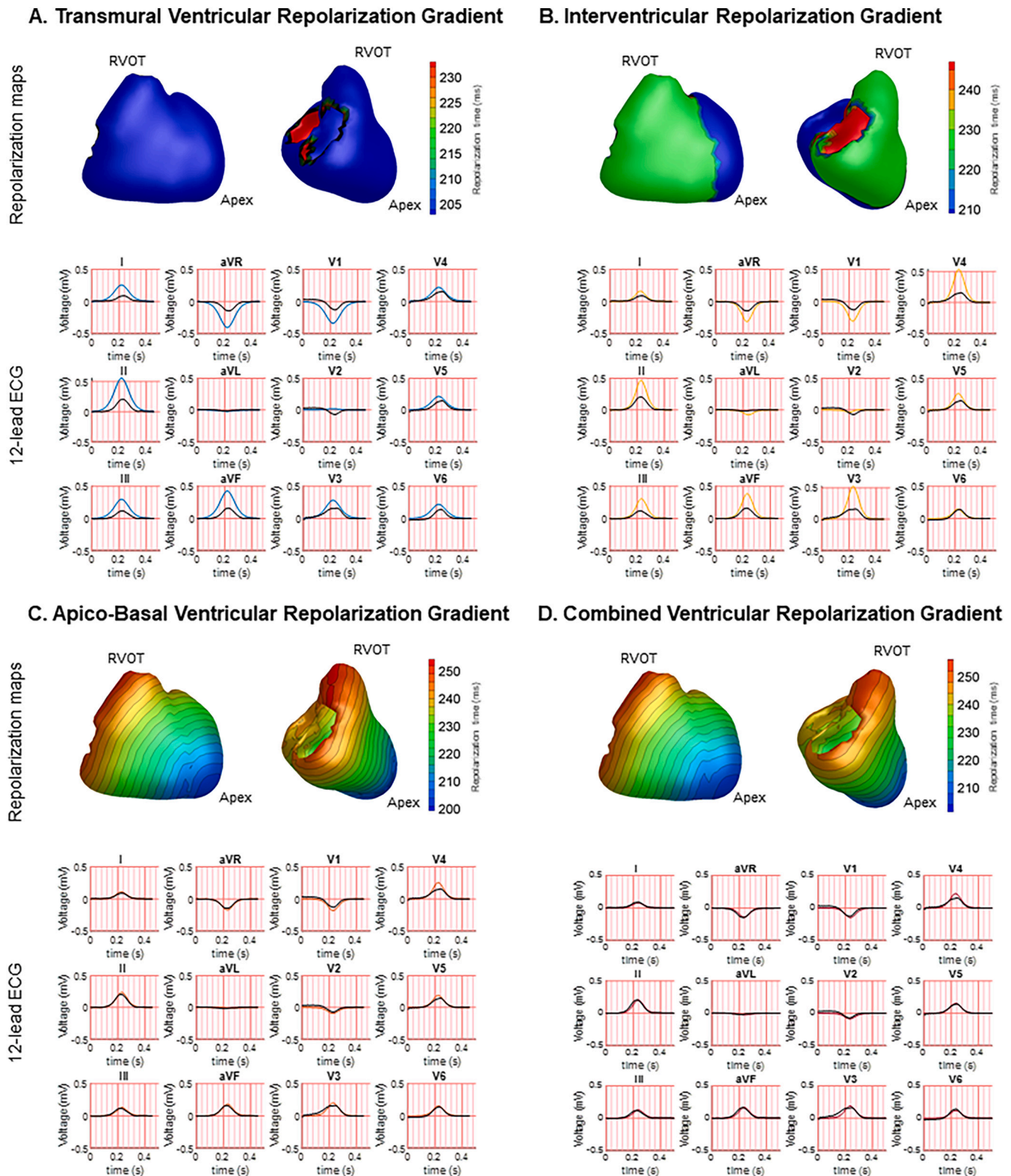


Fig. 1. Effect of ventricular repolarization gradients on T-wave morphology in case 05 (Table 1). The ventricular repolarization maps are displayed in the top row of panel A-E. The 12-lead ECG (obtained from the 67-electrode body surface potential mapping) is presented in the bottom row of panel A-E. The black signal represents measured T-waves, the blue signal simulated T-waves for a transmural ventricular repolarization gradient, the yellow signal simulated T-waves for an interventricular repolarization gradient, the orange signal simulated T-waves for an apico-basal ventricular repolarization gradient, the red signal simulated T-waves for a combined ventricular repolarization gradient and the green signal simulated T-waves for a combined ventricular repolarization gradient after optimization*. (*Repolarization times were optimized using a dedicated Levenberg-Marquardt algorithm with the regularization parameter μ set at e-6). (For interpretation of the references to colour in this figure legend, the reader is referred to the web version of this article.)

E. Combined Ventricular Repolarization Gradient*

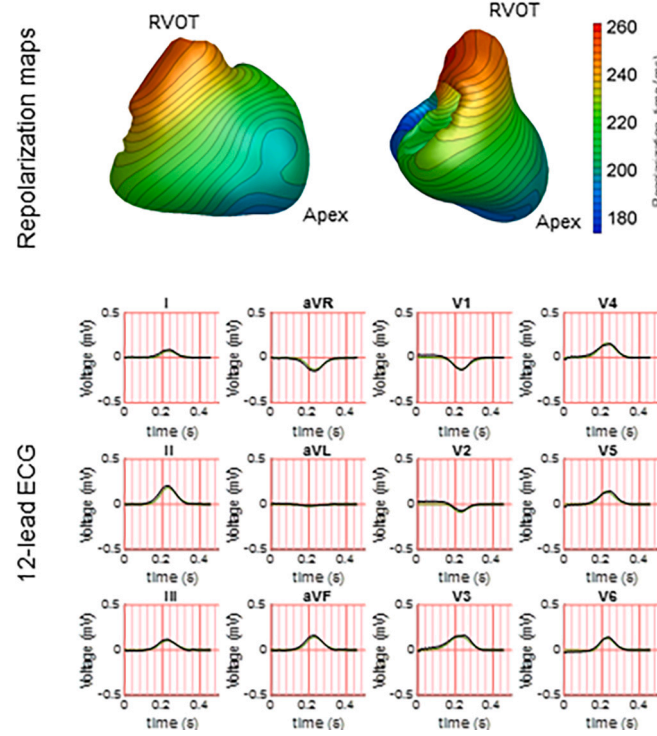


Fig. 1. (continued).

equivalent dipole layer (EDL), a cardiac source model based on transmembrane potentials, with the aim to better understand the relationship between ventricular repolarization gradients and T-wave morphology. [7]

Methods

Study population.

The study population consists of subjects who were clinically referred for cardiac magnetic resonance imaging (CMR) in the University Medical Center Utrecht. Subjects were included in this study if no functional or structural heart disease was present at echo/CMR, no cardiovascular diseases or risk factors were present and QRS duration was <120 ms. The study was approved by the local institutional ethics review board at University Medical Center Utrecht (ID: 17/628).

BSPM signal acquisition and processing.

Each subject underwent 67-electrode body surface potential mapping (BSPM) (sampling frequency: 2048 Hz, Biosemi, Amsterdam, The Netherlands) within 32 days before/after CMR. BSPM were recorded for approximately five minutes with the patient in resting supine position.

BSPM signals were loaded into MATLAB (R2019B) for offline processing and signal analysis. Signals were down sampled to 1000 Hz, high-pass filtered ($f_c = 0.25$ Hz), low-pass filtered ($f_c = 200$ Hz) and notch filtered (50 Hz). Ten beats with the most identical morphology and maximal RS amplitude (assumed end-expiration) were selected and used to compute a median beat. The root mean square (RMS) signal was used to manually annotate the beginning of depolarization (QRS_{onset}), the end of depolarization (QRS_{end}) and the end of repolarization (T_{end}). Leads containing electrode motion artefacts were removed or linearly interpolated.

Cardiac imaging acquisition and processing.

Segmentation of obtained CMR was performed on cardiac short-axis and long-axis cine CMR images at end diastole. Per subject, a 3D-model was created of the ventricular myocardium, blood pools, thorax and

lungs with the following assigned conductivities: 0.2 S/m, 0.6 S/m, 0.4 S/m and 0.2 S/m respectively. Images were segmented using dedicated software (GeomPeacs, Version 0.1.1.4408, Peacs Investments BV) and discretized as closed triangulated surface meshes bounding the segmented mass. Right ventricular, left ventricular, endocardial, epicardial and septal nodes were specified. [8] Lead positions were captured using a 3D camera during the BSPM and registered to the torso model (PeacsCamera, Version 0.02.4979, Peacs Investments BV). [9]

Equivalent dipole layer based T-wave simulations.

The boundary element method was used to compute the transfer matrix to account for the volume conductor effects. [7] The volume conductor model was then used with the EDL as a cardiac source model to compute the electrical potentials at the body surface. The source strength at each ventricular node of the EDL was defined by the shape of the transmembrane potential and was set to 40 mV. [7] The shape of the transmembrane potential was modified to investigate the effect of ventricular repolarization gradients on T-wave morphology. Transmural, interventricular, apico-basal and combined ventricular repolarization gradients were applied (Fig. 1, panel A-E). The correspondence between simulated and measured T-waves was assessed using the correlation coefficient (CC) and relative difference (RD). On a group level, values were presented as median (Q1 Q3).

The normalized shape of the transmembrane potential (V_m) was determined by the multiplication of a linear line with a sigmoid curve [10], representing the plateau phase and repolarization phase respectively:

$$V_m(t) = (V_{dep} + at) * \frac{1}{1 + e^{R(t-T_{rep})}} \quad (1)$$

With V_{dep} the membrane potential at the end of depolarization set at 1, a the downslope of the linear line set at -0.00001 mV/ms, t the time after the end of depolarization of the simulated transmembrane potential, R the slope of the sigmoid curve and T_{rep} the local repolarization time. The downslope of the linear line was constant for all simulated

ventricular gradients and the slope of the sigmoid curve was optimized based on the highest CC between simulated and measured T-waves.

Ventricular repolarization gradients were created by applying a difference in repolarization times between cardiac regions. A difference in repolarization times was applied between the epicardial, endocardial and septal nodes to simulate the transmural ventricular repolarization gradient. To simulate the interventricular repolarization gradient, a difference in repolarization times between the right ventricular, left ventricular and septal nodes was applied. For the apico-basal ventricular gradient, a node on the epicardial apical region was selected and repolarization times increased - depending on their geodesic distance to the apex - towards the base. The selected node in the apical region was determined by the best fit (highest CC) between simulated and measured T-waves. The difference in repolarization times (amount of ventricular repolarization gradient) was also determined by the best fit (highest CC) between simulated and measured T-waves.

For the combined ventricular repolarization gradient, the ventricular repolarization gradient with the best fit (highest CC) was used as a basis and the other two ventricular repolarization gradients were added until the best fit (highest CC) was reached. The output (repolarization times at each node at the ventricular surface) of this algorithm was further optimized using a dedicated Levenberg-Marquardt algorithm using regularization parameter set at $\mu = 10^{-6}$. [11,12] For all models, T-wave correspondence (CC) per lead was determined to create a colour-coded map to identify leads with a bad match between simulated and measured T-waves.

Results

Study population.

The study population consisted of nine individuals, of whom five females and four males, with a median age of 41 years (IQR 30–58) and a median QRS duration of 92 ms (IQR 85–96). Of these nine subjects, seven subjects were diagnosed with premature ventricular complexes originating from the right ventricular outflow tract (RVOT-PVC) and two subjects were recreational athletes. None of the subjects had detectable structural or functional heart disease on CMR.

Ventricular repolarization gradients in the genesis of the T-wave.

Realistic T-waves could be simulated using:

- a transmural ventricular repolarization gradient (29 ms (28–30 ms)) if repolarization times of the epicardium (198 ms (170–205 ms)) were shorter than the endocardium (202 ms (182–232 ms)) (Fig. 1A).
- an interventricular repolarization gradient (9 ms (3–10 ms)) if repolarization times of the left ventricle (195 ms (187–219 ms)) were shorter than the right ventricle (207 ms (196–229 ms)) (Fig. 1B). In two cases, the repolarization times of the right ventricle were shorter than the left ventricle.

- an apico-basal ventricular repolarization gradient (65 ms (63–68 ms)) if repolarization times increased from apex (180 ms (162–202 ms)) towards base (237 ms (228–257 ms)) (Fig. 1C).

In most cases (Table 1), the highest correspondence between measured and simulated T-waves was observed when applying an apico-basal gradient (CC 0.84 (0.81–0.91); RD 0.68 (0.60–0.71)). In one case, the highest CC (0.86 compared to 0.59 for an interventricular gradient and 0.78 for an apico-basal ventricular gradient) was reached applying a transmural repolarization gradient. In another case, the lowest RD (0.64 compared to 0.88 for an interventricular gradient and 0.71 for an apico-basal ventricular gradient) was reached applying a transmural repolarization gradient. Overall, the interventricular gradient resulted in the poorest waveform match (lowest CC) between measured and simulated T-waves (0.71 (0.67–0.80) compared to 0.77 (0.71–0.80) for a transmural gradient and 0.84 (0.81–0.91) for an apico-basal gradient). The transmural gradient resulted in the poorest amplitude match (RD) between measured and simulated T-waves (1.46 (0.82–1.75) compared to 0.85 (0.75–0.87) for an interventricular gradient and 0.68 (0.60–0.71) for an apico-basal gradient).

As the apico-basal gradient resulted in the best match between measured and simulated T-waves, we used the apico-basal ventricular repolarization gradient as a basis. The apico-basal ventricular repolarization gradient was combined (Table 2) with the interventricular repolarization gradient (1 ms (0–1 ms)) and transmural ventricular repolarization gradient (–2 ms (–7–1 ms)). Combining all three gradients resulted in a similar CC 0.83 (0.82–0.89) but a reduced RD 0.60 (0.51–0.63) compared to a sole apico-basal repolarization gradient (CC 0.84 (0.81–0.91); RD 0.68 (0.60–0.71)). Finally, the best correspondence between the measured T-waves versus simulated T-waves was reached after optimization (CC 0.96 (0.94–0.98); RD 0.27 (0.22–0.34)).

Ventricular repolarization gradients and T-wave correspondence per lead.

The highest correspondence between simulated and measured T-waves was reached for electrodes on the right superior part of the chest and the left inferior part of the chest (Fig. 2). The lowest correspondence

Table 2

Ventricular repolarization gradients (ms) in all cases.

	Transmural	Interventricular	Apex-base	Combined Transmural Interventricular	
Case 01	27	9	63	–6	0
Case 02	30	1	65	–8	2
Case 03	30	9	63	–2	1
Case 04	28	3	68	–8	1
Case 05	29	10	55	1	–1
Case 06	30	6	68	–7	5
Case 07	29	2	66	0	0
Case 08	30	20	76	–1	0
Case 09	23	12	57	–1	1

Table 1

Ventricular repolarization gradients and T-wave correspondence between measured and simulated T-waves.

	Repolarization gradients									
	Transmural		Interventricular		Apico-Basal		Combined		Combined + Optimized	
	CC	RD	CC	RD	CC	RD	CC	RD	CC	RD
Case 01	0.86	0.82	0.59	0.87	0.78	0.69	0.83	0.60	0.94	0.34
Case 02	0.77	0.73	0.68	0.90	0.81	0.72	0.82	0.63	0.98	0.20
Case 03	0.67	1.46	0.71	0.75	0.89	0.51	0.88	0.49	0.93	0.37
Case 04	0.84	0.64	0.80	0.88	0.84	0.71	0.83	0.62	0.94	0.34
Case 05	0.73	4.02	0.87	0.61	0.91	0.60	0.90	0.53	0.96	0.29
Case 06	0.71	0.90	0.76	0.85	0.92	0.68	0.89	0.51	0.98	0.22
Case 07	0.79	2.51	0.67	0.86	0.81	0.68	0.82	0.67	0.97	0.26
Case 08	0.66	1.75	0.61	0.84	0.76	0.72	0.77	0.71	0.96	0.27
Case 09	0.80	1.52	0.82	0.67	0.93	0.42	0.94	0.38	0.98	0.20

CC = correlation coefficient, RD = relative difference.

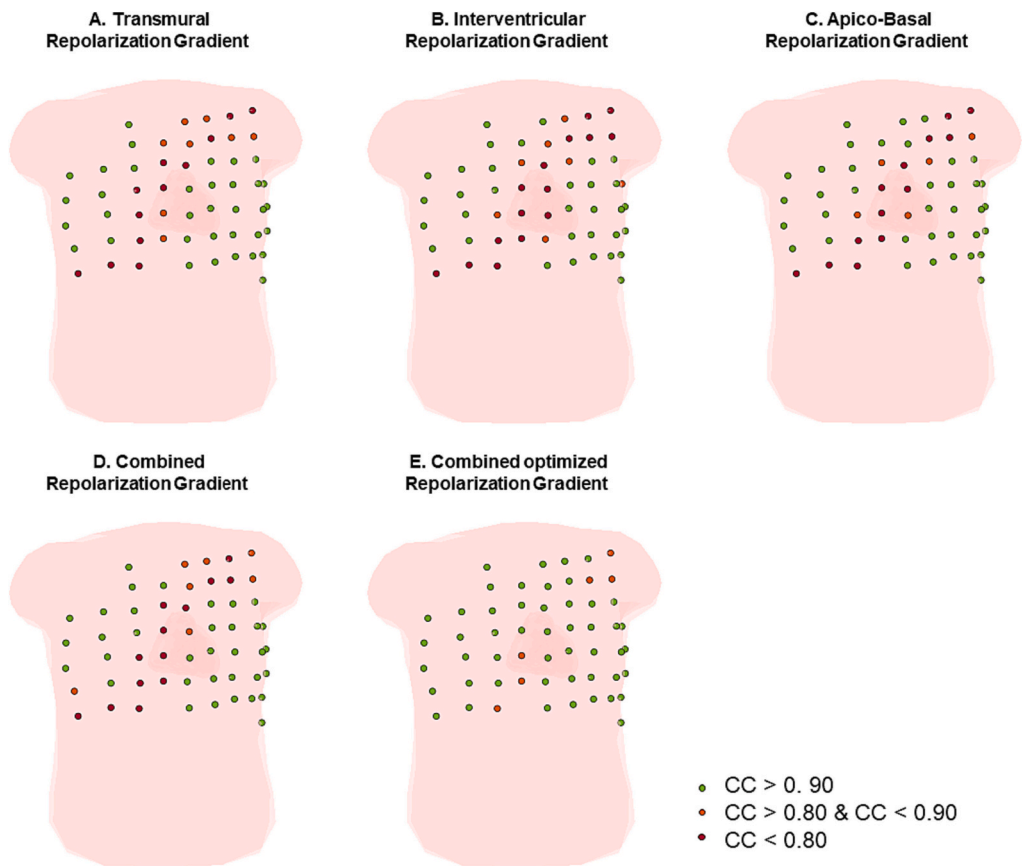


Fig. 2. Ventricular repolarization gradients and median T-wave correspondence between measured and simulated T-waves per lead. The median correspondence (CC = correlation coefficient) between simulated and measured T-waves is displayed on a heart and torso model per lead in panel: A.) transmural ventricular repolarization gradient, B.) interventricular repolarization gradient, C.) apico-basal ventricular repolarization gradient, D.) combined ventricular repolarization gradient and E.) combined optimized repolarization gradient. The colours of the electrodes indicate the degree of correspondence (green = high (CC > 0.90), yellow = moderate (CC > 0.80 & CC < 0.90) and red = poor (CC < 0.80)). (For interpretation of the references to colour in this figure legend, the reader is referred to the web version of this article.)



Fig. 3. Body surface potential map (BSPM) of the precordial leads (positioned as indicated in Fig. 2) of case 08 (Table 1). The black signal represents measured T-waves, the red signal simulated T-waves for the combined optimized ventricular repolarization gradient (correlation coefficient = 0.96; relative difference = 0.27). (For interpretation of the references to colour in this figure legend, the reader is referred to the web version of this article.)

between simulated and measured T-waves was found in a diagonal line from the right inferior part of the chest towards the left superior part of the chest, corresponding with low amplitude T-waves (Fig. 3).

Discussion

This study used the EDL as a cardiac source model to investigate the effect of ventricular repolarization gradients on T-wave morphology. The results in this study indicate that an apico-basal ventricular repolarization gradient plays a dominant role in T-wave formation as the highest correspondence between simulated and measured T-waves was reached when an apico-basal repolarization gradient was applied. The combination of an apico-basal ventricular gradient with an interventricular gradient and transmural ventricular gradient, however, resulted in an increased match between the simulated and measured T-waves, indicating that all three gradients are needed to simulate realistic T-waves.

Transmural ventricular repolarization gradient.

Realistic T-waves could be simulated for the transmural ventricular repolarization gradient if repolarization times of the epicardium were shorter than the endocardium. This is in concordance with studies on intact human hearts, findings in wedge preparations and other computer simulations. [4,5] [13] Application of a transmural repolarization gradient resulted in realistic T-wave shapes (CC 0.77 Table 1) but in inaccurate T-wave amplitudes (RD 1.46 Table 1). A median gradient of 29 ms (28–30 ms) was applied to reach the best match between measured and simulated T-waves. A repolarization gradient of 29 ms is in accordance with a study by Glukhov et al. where they found a repolarization gradient of 30 ms in wedges from human hearts. [14] In a computational study by Weiss et al., similar transmural repolarization gradients were applied as well (9 to 54 ms). [13].

Interventricular repolarization gradient.

In the current study, when applying the interventricular repolarization gradient, realistic T-waves could be simulated if repolarization times of the right ventricle were longer than the left ventricle. Only a small gradient was applied of 9 ms (3–10 ms). The interventricular gradient resulted in the poorest waveform match between measured and simulated T-waves, when compared to the transmural and apico-basal gradients (Table 1). A clear comparison with literature could not be made because more diffuse patterns of repolarization on both the left and right ventricle were observed in whole heart studies and other simulation studies. [3,6,13,15,16]

Apico-basal repolarization gradient.

In our study, the application of an apico-basal ventricular repolarization gradient resulted in realistic T-waves if repolarization times increased from apex towards base. Apico-basal gradients have been described in literature, but the described ventricular gradients are contradictory. Longer action potential durations (APD) have been described in both the base compared to the apex and the apex compared to the base. [4,6,13] An apico-basal ventricular repolarization gradient was also described by van Dam et al. using CineECG in 6500 normal cases. [17] In this study, the PathECG during repolarization was directed from the base towards the apex. However, the electrical gradient during repolarization – the repolarization sequence – is opposite to the vector derived pathECG direction. Thus, an apico-basal ventricular repolarization gradient was also found using CineECG. In our study, an apico-basal ventricular repolarization gradient resulted in the best match between simulated and measured T-waves compared to a transmural and interventricular repolarization gradient. Similar results were obtained in a study by Xue et al. They used a GE cell-to-electrocardiogram model and found that the apico-basal dispersion of repolarization contributed more to positive T-waves than a transmural dispersion. [18]

Combined ventricular repolarization gradients.

The combination of an apico-basal ventricular gradient with an interventricular gradient and transmural ventricular gradient resulted in the best match between simulated and measured T-waves. The results

therefore indicate that all three gradients are important in the genesis of the T-wave. The intra-variability for the transmural gradient (Table 2) was small whereas the intra-variability for the interventricular and apico-basal gradient were larger. A larger transmural gradient was applied compared to the interventricular gradient when all three gradients were combined. Overall, there were some slightly subject-to-subject differences. This was also indicated in several other studies where a diffuse pattern of repolarization times was observed over the ventricular wall and thereby also different ventricular repolarization gradients. [3,5,19] In addition, a study by Opthof et al. in three donor hearts found a bigger difference in repolarization patterns compared to activation patterns. The total repolarization time, the start locations of the repolarization sequence, the end locations of the repolarization sequence and the resulting repolarization gradients were found to be different among the donor hearts. [19] Indicating that not one repolarization gradient is responsible for the genesis of the T-wave but, a complex interplay of different ventricular repolarization gradients.

Limitations and future directions.

A limitation of this study is not including the activation sequence as a starting point for the repolarization sequence as the repolarization sequence is determined by the APD and the activation sequence. The activation sequence was not included in this study because we aimed to model solely the repolarization sequence to improve our EDL-based inverse procedure. In future studies, the best estimate of the depolarization sequence [11] will be combined with the best estimate of the repolarization sequence to make a final computation for the complete QRST-complex.

Another limitation is the control population, as most subjects were diagnosed with RVOT-PVC. Although no detectable structural or functional heart disease was observed with CMR, repolarization times may be different in the RV/RVOT area. In a future study, we will compare our EDL-based inverse with invasive mapping studies to validate our model.

Future studies will also focus on the template of the transmembrane potential. Deviated ST-segments could not be simulated accurately using the current template (Eq. 1, Fig. 3). In addition, biphasic T-waves and low amplitude T-waves were also not adequately simulated (Figs. 2 and 3). Therefore, the template of the transmembrane potential should be further parametrized. For example, the downslope of the linear line may be an important parameter to optimize during the inverse procedure. When normal repolarization can be modeled adequately, the EDL will be used to better understand STT-wave abnormalities in for example cardiac ischemia and cardiomyopathies.

Conclusion

This study showed the ability of the EDL cardiac source model to simulate realistic T-waves. The results indicate that the apico-basal repolarization gradient plays a dominant role in T-wave formation. A combination of an interventricular, transmural and apico-basal gradient further improved the simulated T-waves, indicating that all three gradients are required in the genesis of the T-wave. The work performed in this study will be used to optimize our EDL-based inverse ECG procedure to assess repolarization abnormalities.

Acknowledgements

We would like to thank A.P.M. Gorgels for his constructive discussion and review.

Funding

This project was supported by the Dutch Heart Foundation grant numbers: QRS-Vision 2018B007 and STT-Vision 2020B010.

Conflict of interest

Peter van Dam is an owner of ECG Excellence BV / Peacs BV.
Author Statement.

M. Kloosterman: Conceptualization, methodology, software, formal analysis, investigation, writing – original draft, visualization **M.J. Boonstra:** Investigation, writing – review & editing **I. van der Schaaf:** Writing – review & editing **P. Loh:** – writing: Review & editing, supervision **P.M. van Dam:** Conceptualization, methodology, software, writing – review & editing, supervision.

References

- [1] Das MK, et al. Fragmented QRS on twelve-lead electrocardiogram predicts arrhythmic events in patients with ischemic and nonischemic cardiomyopathy. *Hear Rhythm* 2010;7(1):74–80.
- [2] Istolahti T, et al. The prognostic significance of T-wave inversion according to ECG lead group during long-term follow-up in the general population. *Ann Noninvasive Electrocardiol* 2021;26(1):1–9.
- [3] Meijborg VMF, Conrath CE, Opthof T, Belterman CNW, De Bakker JMT, Coronel R. Electrocardiographic T wave and its relation with ventricular repolarization along major anatomical axes. *Circ. Arrhythmia Electrophysiol.* 2014;7(3):524–31.
- [4] Patel C, et al. Is there a significant transmural gradient in repolarization time in the intact heart?: cellular basis of the T wave: a century of controversy. *Circ Arrhythmia Electrophysiol* 2009;2(1):80–8.
- [5] Artyeva NV. Dispersion of ventricular repolarization: temporal and spatial. *World J Cardiol* 2020;12(9):437.
- [6] Opthof T, Janse MJ, Meijborg VMF, Cinca J, Rosen MR, Coronel R. Dispersion in ventricular repolarization in the human, canine and porcine heart. *Prog Biophys Mol Biol* 2016;120(1–3):222–35.
- [7] Oostendorp T, Van Oosterom A. The potential distribution generated by surface electrodes in inhomogeneous volume conductors of arbitrary shape. *IEEE Trans Biomed Eng* 1991;38(5):409–17.
- [8] van Dam P, Gordon J, Laks M, Boyle N. Development of new anatomy reconstruction software to localize cardiac isochrones to the cardiac surface from the 12 lead ECG. *J Electrocardiol* 2015;48(6):959–65.
- [9] Samir A, Kastelein M, van Dam E, van Dam P. Automatic registration of 3D camera recording to model for leads localization. *Comput Cardiol* 2017;44:1–4.
- [10] Van Oosterom A, Jacquemet V. A parameterized description of transmembrane potentials used in forward and inverse procedures. *Folia Cardiol* 2005;12:111–3.
- [11] Boonstra MJ, et al. Modeling the his-Purkinje effect in non-invasive estimation of endocardial and Epicardial ventricular activation. *Ann Biomed Eng* 2022;50(3):343–59.
- [12] Van Dam PM, Oostendorp TF, Linnenbank AC, Van Oosterom A. Non-invasive imaging of cardiac activation and recovery. *Ann Biomed Eng* 2009;37(9):1739.
- [13] Weiss DL, Ifland M, Sachse FB, Seemann G, Dössel O. Modeling of cardiac ischemia in human myocytes and tissue including spatiotemporal electrophysiological variations. *Biomed Tech* 2009;54(3):107–25.
- [14] Glukhov AV, et al. Transmural dispersion of repolarization in failing and nonfailing human ventricle. *Circ Res* 2010;106(5):981–91.
- [15] Janse MJ, Coronel R, Opthof T, Sosunov EA, Anyukhovsky EP, Rosen MR. Repolarization gradients in the intact heart: transmural or apico-basal? *Prog Biophys Mol Biol* 2012;109(1–2):6–15.
- [16] Opthof T, Coronel R, Janse MJ. Is there a significant transmural gradient in repolarization time in the intact heart?: repolarization gradients in the intact heart. *Circ. Arrhythmia Electrophysiol.* 2009;2(1):89–96.
- [17] van Dam PM, Boonstra M, Locati ET, Loh P. The relation of 12 lead ECG to the cardiac anatomy: the normal CineECG. *J Electrocardiol* 2021;69:67–74.
- [18] Xue J, Chen Y, Han X, Gao W. Electrocardiographic morphology changes with different type of repolarization dispersions. *J Electrocardiol* 2010;43(6):553–9.
- [19] Opthof T, et al. Cardiac activation–repolarization patterns and ion channel expression mapping in intact isolated normal human hearts. *Hear. Rhythm* 2017; 14(2):265–72.